AMSR-E/Aqua Daily L3 6.25 km 89 GHz Brightness Temperature Polar Grids, Version 3

USER GUIDE

How to Cite These Data

As a condition of using these data, you must include a citation:

Author. Date. Cavalieri, D. J., T. Markus, and J. C. Comiso. 2014. *AMSR-E/Aqua Daily L3 6.25 km 89 GHz Brightness Temperature Polar Grids, Version 3.* [Indicate subset used]. Boulder, Colorado USA. NASA National Snow and Ice Data Center Distributed Active Archive Center. https://doi.org/10.5067/AMSR-E/AE_SI6.003. [Date Accessed].

FOR QUESTIONS ABOUT THESE DATA, CONTACT NSIDC@NSIDC.ORG

FOR CURRENT INFORMATION, VISIT https://nsidc.org/data/AE_SI6

NSIDC National Snow and Ice Data Center

TABLE OF CONTENTS

1 DETAILED DATA DESCRIPTION

1.1 Format

Data are stored in Hierarchical Data Format - Earth Observing System (HDF-EOS) format.

1.2 File and Directory Structure

Files contain core metadata, product-specific attributes, and the data fields in 2-byte signed integer format. Missing data values are indicated by 0. Data have a scale factor of 0.1. Multiply data values by 0.1 to obtain brightness temperatures in kelvins (K). The valid range of brightness temperature is approximately 50 to 300 K. Refer to Table 1 and Table 2 for parameter summary information.

Table 1. Northern Hemisphere Parameter Summary

Field Name	Description
SI_06km_NH_89V_ASC	89.0 GHz vertical daily average ascending T_bs
SI_06km_NH_89V_DSC	89.0 GHz vertical daily average descending T_bs
SI_06km_NH_89V_DAY	89.0 GHz vertical daily average T_bs
SI_06km_NH_89H_ASC	89.0 GHz horizontal daily average ascending T_bs
SI_06km_NH_89H_DSC	89.0 GHz horizontal daily average descending T_bs
SI_06km_NH_89H_DAY	89.0 GHz horizontal daily average T_bs

Table 2. Southern Hemisphere Parameter Summary

Field Name	Description
SI_06km_SH_89V_ASC	89.0 GHz vertical daily average ascending T_bs
SI_06km_SH_89V_DSC	89.0 GHz vertical daily average descending T_bs
SI_06km_SH_89V_DAY	89.0 GHz vertical daily average T_bs
SI_06km_SH_89H_ASC	89.0 GHz horizontal daily average ascending T_bs
SI_06km_SH_89H_DSC	89.0 GHz horizontal daily average descending T_bs
SI_06km_SH_89H_DAY	89.0 GHz horizontal daily average T_bs

1.3 File Naming Convention

This section explains the file naming convention used for this product with examples.

Example file names:

AMSR_E_L3_SeaIce6km_V15_20080207.hdf

AMSR_E_L3_SeaIce6km_X##_yyyymmdd.hdf

Refer to Table 3 for the values of the file name variables listed above.

Table 3. Variable Values for the File Name

Variable	Description
`X`	Product Maturity Code (Refer to Table 4 for valid values.)
`##`	file version number
`yyyy`	four-digit year
`mm`	two-digit month
`dd`	two-digit day
`hdf`	Hierarchical Data Format (HDF)

Table 4. Variable Values for the Product Maturity Code

Variables	Description
P	Preliminary - refers to non-standard, near-real-time data available from NSIDC. These data are only available for a limited time until the corresponding standard product is ingested at NSIDC.
B	Beta - indicates a developing algorithm with updates anticipated.
T	Transitional - period between beta and validated where the product is past the beta stage, but not quite ready for validation. This is where the algorithm matures and stabilizes.
V	Validated - products are upgraded to Validated once the algorithm is verified by the algorithm team and validated by the validation teams. Validated products have an associated validation stage. Refer to Table 5 for a description of the stages.

Table 5. Validation Stages

Validation Stage	Description
Stage 1	Product accuracy is estimated using a small number of independent measurements obtained from selected locations, time periods, and ground-truth/field program efforts.
Stage 2	Product accuracy is assessed over a widely distributed set of locations and time periods via several ground-truth and validation efforts.
Stage 3	Product accuracy is assessed, and the uncertainties in the product are well-established via independent measurements made in a systematic and statistically robust way that represents global conditions.

Table 6 provides examples of file name extensions for related files that further describe or supplement data files.

Table 6. Related File Extensions and Descriptions

Extensions for Related Files	Description
`.jpg`	Browse data
`.qa`	Quality assurance information
`.ph`	Product history data
`.xml`	Metadata files

1.4 File Size

Each daily granule is approximately 46 MB.

1.5 Spatial Coverage

1.5.1 Spatial Coverage Map

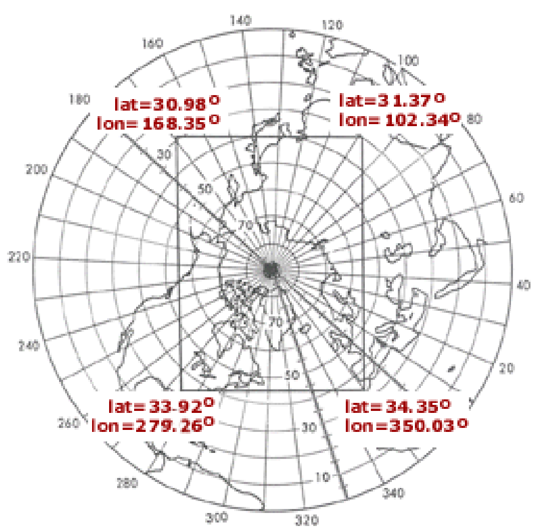

Figure 1. Northern Hemisphere

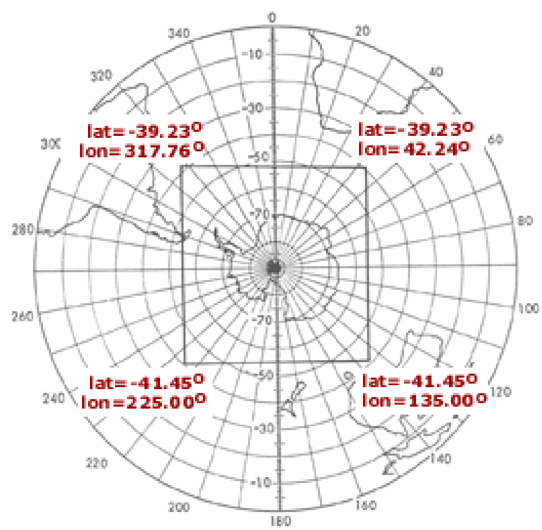

Figure 2. Southern Hemisphere

1.5.2 Spatial Resolution

The 89 GHz observations from the AMSR-E/Aqua L2A Global Swath Spatially-Resampled Brightness Temperatures product have a native 5.4 km resolution.

The spatial resolution of the 89 GHz brightness temperature polar grids are 6.25 km.

1.6 Projection and Grid Description

1.6.1 Projection

Brightness temperature grids are in a polar stereographic projection, which specifies a projection plane such as the grid tangent to the earth at 70 degrees. The planar grid is designed so that the grid cells at 70 degrees latitude are 6.25 km by 6.25 km. For more information on this topic please refer to Pearson (1990) and Snyder (1987).

The polar stereographic projection often assumes that the plane (grid) is tangent to the Earth at the pole. Thus, there is a one-to-one mapping between the Earth's surface and grid with no distortion at the pole. Distortion in the grid increases as the latitude decreases because more of the Earth's surface falls into any given grid cell. At the edge of the northern polar grid distortion reaches 31 percent. The southern polar grid has a maximum distortion of 22 percent. To minimize the distortion, the projection is true at 70 degrees rather than at the poles. This increases the distortion at the poles by three percent and decreases the distortion at the grid boundaries by the same amount. The latitude of 70 degrees was selected so that little or no distortion would occur in the marginal ice zone. Another result of this assumption is that fewer grid cells will be required as the Earth's surface is more accurately represented.

The polar stereographic formula for converting between latitude/longitude and X-Y grid coordinates are taken from Snyder (1982). This projection assumes a Hughes ellipsoid with a radius of 3443.992 nautical mi or 6378.273 km and an eccentricity (e) of 0.081816153 (or e**2 = 0.006693883). The structural metadata (StructMetadata.0) built into the HDF-EOS data file lists the squared eccentricity value rounded to four significant digits (0.006694).

1.6.2 Grid Description

Northern Hemisphere: 1216 columns by 1792 rows
Southern Hemisphere: 1263 columns by 1327 rows

The origin of each x, y grid is the pole. The grids' approximate outer boundaries are defined in Tables 7 and 8. Corner points are listed starting from the upper left and reading clockwise. Interim rows define boundary midpoints.

Table 7. North Polar

X (km)	Y (km)	Latitude (deg)	Longitude (deg)	Pixel Location
-3850	5850	30.98	168.35	corner
0	5850	39.43	135.00	midpoint

X (km)	Y (km)	Latitude (deg)	Longitude (deg)	Pixel Location
3750	5850	31.37	102.34	corner
3750	0	56.35	45.00	midpoint
3750	-5350	34.35	350.03	corner
0	-5350	43.28	315.00	midpoint
-3850	-5350	33.92	279.26	corner
-3850	0	55.50	225.00	midpoint

Table 8. South Polar

X (km)	Y (km)	Latitude (deg)	Longitude (deg)	Pixel Location
-3950	4350	-39.23	317.76	corner
0	4350	-51.32	0.00	midpoint
3950	4350	-39.23	42.24	corner
3950	0	-54.66	90.00	midpoint
3950	-3950	-41.45	135.00	corner
0	-3950	-54.66	180.00	midpoint
-3950	-3950	-41.45	225.00	corner
-3950	0	-54.66	270.00	midpoint

For this EASE-Grid product, there are files that contain geolocation and pixel-area tools, which provide the same functionality for all polar stereographic passive microwave sea ice data sets at NSIDC. These tools include a FORTRAN routine called locate, a latitude/longitude grid, and a pixel-area grid.

The geocoordinate FORTRAN tools available are the following. They are available via FTP.

- **locate.for**: A FORTRAN routine that allows the user to enter an i,j coordinate and get the corresponding latitude/longitude coordinate, and vice versa.
- **mapll.for** and **mapxy.for**: Subroutines that are associated with the locate.for program. These programs need to be compiled, but are not run explicitly. They are called by locate.for. Thus, the user should compile these programs with locate.for and then use locate to do the conversions.

The latitude/longitude grids are in binary format and are stored as long word integers (4 byte) scaled by 100,000. Each array location (i,j) contains the latitude or longitude value at the center of the corresponding data grid cells. These tar files are available via FTP.

Table 9. File Variables

Variables	Description
`pss`	polar stereographic southern projection
`psn`	polar stereographic northern projection
`06, 12, & 25`	6 km, 12 km, and 25 km, respectively
`lat`	latitude grid
`lon`	longitude grid
`area`	pixel area

1.7 Temporal Coverage

Data were collected from 01 June 2002 to 4 October 2011.

1.7.1 Temporal Resolution

Brightness temperatures are composites of daily-averaged ascending orbits, daily-averaged descending orbits and full daily averages.

1.8 Parameter or Variable

Brightness Temperature (T_b)

1.8.1 Parameter Description

Vertical and horizontal brightness temperatures for the 89 GHz channel.

2 SOFTWARE AND TOOLS

For tools that work with AMSR-E data, see the AMSR-E Web page.

3 DATA ACQUISITION AND PROCESSING

3.1 Data Source

The 89 GHz observations at 5.4 km resolution from the AMSR-E/Aqua L2A Global Swath Spatially-Resampled Brightness Temperatures product are gridded to a 6.25 km polar stereographic grid using a drop-in-the-bucket approach where the grid cell that contains the center of the observation footprint is given the whole weight of the observation. All valid observations within the extent of the polar grids are binned into grid cells including land observations.

3.2 Derivation Techniques and Algorithms

Refer to the AMSR-E/Aqua L2A Global Swath Spatially-Resampled Brightness Temperatures guide document for details of calculating AMSR-E brightness temperatures.

Beginning with version 3, the Southern Hemisphere sea ice concentration algorithm no longer uses the Level-2A land flag and only uses the updated land mask for surface type classification.

3.2.1 Processing Steps

Swath data from the 89 GHz channel are mapped onto the 6.25 km polar stereographic grid by converting the geodetic latitude and longitude for the center of each scene station, such as the observation footprint, into AMSR-E map grid coordinates. Scene station map grid coordinates determine grid cell assignments. Observations falling outside the AMSR-E polar grid are ignored. For each grid cell, brightness temperatures observed over a 24-hour period (midnight to midnight GMT) are summed and then divided by the total observations to obtain a daily-average brightness temperature value. If no observations fall within a grid cell for a given day, the average brightness temperature is labeled missing.

After input Level-2A brightness temperatures are binned into 6.25 km grid cells, the ascending, descending, and daily data are averaged. Refer to the Data Source section of this guide document for more information. The daily average is not simply an average of ascending and descending orbits, because a given pixel could have, for example, three measurements from ascending orbits and two from descending orbits. Instead, the daily average is of all the observations for that grid cell. For example, if A = ascending and B = descending:

$$\frac{\frac{A1+A2}{2}+\frac{B1+B2+B3}{3}}{2} \qquad \textbf{(Equation 1)}$$

is not equal to:

$$\frac{A1+A2+B1+B2+B3}{5} \qquad \textbf{(Equation 2)}$$

However, this biases daytime (ascending) orbits over nighttime (descending)

3.2.1.1 Land Masks

The AMSR-E sea ice product utilizes a 6.25 km Northern Hemisphere land mask (amsr_gsfc_6n.hdf) and a 6.25 km Southern Hemisphere land mask (amsr_nic_6s.hdf). The North land mask has not been updated since 1997. The South land mask for includes an updated ice shelf definition created by the National Ice Center Science Department in June 2011 and an updated shoreline developed from ENVISAT and RADARSAT imagery from October 2009 to April 2010.

A 1-byte integer array is included in each HDF file.

amsr_gsfc_6n.hdf: 1216 columns x 1792 rows
Values are 0 (water), 3 (coast), 216 (land)
amsr_nic_6s.hdf: 1264 columns x 1328 rows
Values are 0 (water), 1 (land), 2 (coast)

3.2.2 Version History

Changes to the Version 3 (V15-stage 1) algorithm for these data include:

- Use of the most recent version (Version 3) of the AMSR-E/Aqua L2A Global Swath Spatially-Resampled Brightness Temperatures data as input
- An improved Antarctic land mask
- No longer uses the Level-2A land flag and only uses the updated land mask for surface type classification in the Southern Hemisphere sea ice concentration algorithm
- Inclusion of ISO lineage metadata

Refer to the AMSR-E Data Versions web page for a summary of changes since the start of mission.

3.3 Quality Assessment

Each HDF-EOS file contains core metadata with Quality Assessment (QA) metadata flags that are set by the Science Investigator-led Processing System (SIPS) at the Global Hydrology and Climate Center (GHCC) prior to delivery to NSIDC. A separate metadata file in XML format is also delivered to NSIDC with the HDF-EOS file; it contains the same information as the core metadata. Three levels of QA are conducted with the AMSR-E Level-2 and -3 products: automatic, operational, and science QA. If a product does not fail QA, it is ready to be used for higher-level processing, browse generation, active science QA, archive, and distribution. If a granule fails QA, SIPS does not send the granule to NSIDC until it is reprocessed. Level-3 products that fail QA are never delivered to NSIDC (Conway 2002).

3.3.1 Automatic QA

Out-of-bounds Level-2A brightness temperatures are screened out before brightness temperatures are interpolated to the 6.25 km grid.

3.3.2 Operational QA

AMSR-E Level-2A data arriving at GHCC are subject to operational QA prior to processing higher-level products. Operational QA varies by product, but it typically checks for the following criteria in a given file (Conway 2002):

- File is correctly named and sized
- File contains all expected elements
- File is in the expected format
- Required EOS fields of time, latitude, and longitude are present and populated
- Structural metadata is correct and complete
- The file is not a duplicate
- The HDF-EOS version number is provided in the global attributes
- The correct number of input files were available and processed.

3.3.3 Science QA

AMSR-E Level-2A data arriving at GHCC are also subject to science QA prior to processing higher-level products. If less than 50 percent of a granule's data is good, the science QA flag is marked suspect when the granule is delivered to NSIDC. In the SIPS environment, the science QA includes checking the maximum and minimum variable values, and percent of missing data and out-of-bounds data per variable value. At the Science Computing Facility (SCF), also at GHCC, science QA involves reviewing the operational QA files, generating browse images, and performing the following additional automated QA procedures (Conway 2002):

- Historical data comparisons
- Detection of errors in geolocation
- Verification of calibration data
- Trends in calibration data
- Detection of large scatter among data points that should be consistent.

Geolocation errors are corrected during Level-2A processing to prevent processing anomalies such as extended execution times and large percentages of out-of-bounds data in the products derived from Level-2A data.

The Team Lead SIPS (TLSIPS) developed tools for use at SIPS and SCF for inspecting the data granules. These tools generate a QA browse image in Portable Network Graphics (PNG) format and a QA summary report in text format for each data granule. Each browse file shows Level-2A and Level-2B data. These are forwarded from Remote Sensing Systems (RSS) to GHCC along with associated granule information where they are converted to HDF raster images prior to delivery to NSIDC.

Refer to AMSR-E Validation Data for information about data used to check the accuracy and precision of AMSR-E observations.

Refer to the AMSR-E Data Quality document for more information on quality assessment

3.3.4 Error Sources

See the AMSR-E/Aqua L2A Global Swath Spatially-Resampled Brightness Temperatures guide document for information about potential errors with constructed brightness temperatures.

3.4 Sensor or Instrument Description

See the AMSR-E Instrument Description document.

4 REFERENCES AND RELATED PUBLICATIONS

Cavalieri, D. and J. Comiso. 2000. Algorithm Theoretical Basis Document for the AMSR-E Sea Ice Algorithm, Revised December 1. Landover, Maryland USA: Goddard Space Flight Center.

Cavalieri, D. J., K. M. St. Germain, and C. T. Swift. 1995. Reduction of Weather Effects in the Calculation of Sea Ice Concentration with the DMSP SSM/I. *Journal of Glaciology* 41(139): 455-464.

Cavalieri, D. J., P. Gloersen, and W. J. Campbell. 1984. Determination of Sea Ice Parameters with the NIMBUS-7 SMMR. *Journal of Geophysical Research* 89(D4): 5355-5369.

Comiso, J., D. Cavalieri, and T. Markus. 2003. Sea Ice Concentration, Ice Temperature, and Snow Depth using AMSR-E data. *IEEE Transactions on Geoscience and Remote Sensing* 41(2): 243-252.

Comiso, J. and K. Steffen. 2001. Studies of Antarctic Sea Ice Concentrations from Satellite Data and Their Applications. *Journal of Geophysical Research* 106(C12): 31,361-31,385.

Comiso, J. C. 1995. *SSM/I Ice Concentrations Using the Bootstrap Algorithm*. NASA RP 1380.

Conway, D. 2002. *Advanced Microwave Scanning Radiometer - EOS Quality Assurance Plan*. Huntsville, AL: Global Hydrology and Climate Center.

Gloersen P. and D. J. Cavalieri. 1986. Reduction of Weather Effects in the Calculation of Sea Ice Concentration from Microwave Radiances. *Journal of Geophysical Research* 91(C3): 3913-3919.

Kummerow, C. 1993. On the Accuracy of the Eddington Approximation for Radiative Transfer in the Microwave Frequencies. *Journal of Geophysical Research* 98: 2757-2765.

Markus, T., D. Cavalieri, and A. Ivanoff. 2011. Algorithm Theoretical Basis Document for the AMSR-E Sea Ice Algorithm, Revised December 2011. Landover, Maryland USA: Goddard Space Flight Center. (PDF file, 528 KB)

Markus, Thorsten and Donald J. Cavalieri. 2008. [Supplement] AMSR-E Algorithm Theoretical Basis Document: Sea Ice Products. Greenbelt, Maryland USA: Goddard Space Flight Center. (PDF file, 2.10 MB)

Markus, Thorsten and Donald J. Cavalieri. 1998. Snow Depth Distribution over Sea Ice in the Southern Ocean from Satellite Passive Microwave Data. IN: *Antarctic Sea Ice: Physical Processes, Interactions, and Variability*. *Antarctic Research Series* 74:19-39. Washington, DC, USA: American Geophysical Union.

Markus, T. and D. Cavalieri. 2000. An Enhancement of the NASA Team Sea Ice Algorithm. *IEEE Transactions on Geoscience and Remote Sensing* 38: 1387-1398.

Pearson, F. 1990. *Map projections: Theory and Applications*. Boca Raton, FL: CRC Press.

Snyder, J.P. 1987. *Map projections - a Working Manual*. U.S. Geological Survey Professional Paper 1395. U.S. Government Printing Office. Washington, D.C.

Snyder, J. P. 1982. *Map Projections Used by the U.S. Geological Survey.* U.S. Geological Survey Bulletin 1532.

For more information regarding related publications, see the Published Research Web page.

4.1 Related Data Collections

Sea Ice Products at NSIDC

This site offers a complete summary of sea ice data derived from passive microwave sensors and other sources, and is useful for users who want to compare characteristics of various sea ice products to understand their similarities and differences. This site also provides links to tools for passive microwave data and a list of other sea ice resources.

Sea Ice Trends and Climatologies from SMMR and SSM/I-SSMIS

This site provides a suite of value-added products to aid in investigations of the variability and trends of sea ice cover. These products provide users with information about sea ice extent, total ice covered area, ice persistence, monthly climatologies of sea ice concentrations, and ocean masks.

4.2 Related Web Sites

Sea Ice Remote Sensing at NASA/Goddard Space Flight Center

5 CONTACTS AND ACKNOWLEDGMENTS

Donald J. Cavalieri
Laboratory for Hydrospheric Processes
NASA Goddard Space Flight Center

Josefino Comiso
Laboratory for Hydrospheric Processes
NASA Goddard Space Flight Center

Thorsten Markus
Laboratory for Hydrospheric Processes
NASA Goddard Space Flight Center

6 DOCUMENT INFORMATION

6.1 Publication Date

May 2014

6.2 Date Last Updated

21 April 2021